PHYSICAL REVIEW A **85**, 023416 (2012)

Theoretical study of angular-resolved two-photon ionization of H_2

Ph. V. Demekhin,[1,*] B. M. Lagutin,[2] and I. D. Petrov[2]
[1]*Theoretische Chemie, Physikalisch-Chemisches Institut, Universität Heidelberg, Im Neuenheimer Feld 229, DE-69120 Heidelberg, Germany*
[2]*Rostov State Transport University, Narodnogo Opolcheniya Square 2, 344038 Rostov-on-Don, Russia*

(Received 17 January 2012; published 21 February 2012)

Cross sections and angular distribution parameters of electrons ejected via two-photon ionization of the hydrogen molecule by linearly and circularly polarized light are computed in the exciting-photon energy range of 8–14 eV, which covers the first four optical resonant states of the molecule. Photoelectron partial waves in the continuous spectrum are obtained within the single center method in precise numerical potential of the molecular ion field. The correlation function technique is used to calculate the two-photon transition matrix element. The presently computed angular-resolved spectra are in good agreement with the theoretical results available for the photon energy of 8.854 eV and can be considered as reliable predictions in the respective energy range.

DOI: 10.1103/PhysRevA.85.023416 PACS number(s): 32.80.Rm, 33.20.Xx, 82.50.Pt

I. INTRODUCTION

Multiphoton ionization (MPI) of molecules is a well-established branch of spectroscopy that has a substantial body of literature (see, e.g., selected reviews [1–6] and references therein). On the one hand, entirely new states are seen in MPI spectra of molecules. This provides a more complete understanding of electronic structure, complementary to that accessible to single-photon ionization spectroscopy. On the other hand, MPI spectroscopy provides new tools for revisiting known phenomena with higher accuracy and also for investigating new classes of phenomena in molecules. These advantages have placed MPI spectroscopy among the most important experimental tools for studying molecules.

In contrast to a large variety of contemporary experiments on MPI of molecules, there are much less theoretical works on the subject, especially if it concerns angular-resolved studies of molecular MPI. The main difficulties for theoretical calculations are connected both with the noncentral field of a molecule and the need to perform summations over the complete set of intermediate eigenstates, including the continuous spectrum. In addition, an accurate theoretical description of the partial electron continuum waves with given angular momentum quantum numbers is required for studying MPI angular distributions. Here, standard quantum chemistry methods [e.g., molecular-orbital linear combination of atomic orbitals (MO LCAO)] are unfit. Therefore, considerable efforts have been invested to the development of theoretical methods and computational approaches for studying MPI of molecules.

To be concise, only a few of the relevant alternative approaches and applications are mentioned below. In Refs. [7,8], the Green's-function approach for the quantum-defect method was formulated in spheroidal coordinates and applied to study angular-resolved MPI spectra of H_2 and of the H_2^+ ion. Another approach, involving Green's-function and numerical partial harmonics for electron orbitals coupled by the molecular noncentral field, was applied in Ref. [9] to study angular-resolved MPI spectra of H_2. A unified R-matrix-Floquet theory with the standard multicenter electron molecule scattering potential and single center (SC) atomic multiphoton propagator was utilized in Ref. [10] to compute MPI rates of H_2. In Refs. [11,12], MPI spectra of the H_2^+ ion were computed by the numerical Green's functions in prolate spheroidal coordinates using the $\mathcal{L}^2$-integrable B-spline basis set. Finally, a somewhat similar B-spline technique was used in Refs. [13,14] to compute MPI cross sections for differently oriented H_2 and H_2^+.

In spite of quite a number of theoretical studies of MPI of the H_2 molecule mentioned above, the angular-resolved MPI of molecules is still not sufficiently scrutinized. Recently [15,16], we have developed a powerful computational tool for ionization and electronic excitation studies of molecules. It is known as the single center method [17,18], and allows for an accurate theoretical description of excited discrete and partial photoelectron wave continuous functions of molecules. It is especially designed to investigate angular-resolved molecular ionization processes and was already successfully applied to study angular distributions of photoelectrons and fluorescent photons in diatomics [19–22].

In this work we demonstrate that the SC method allows also a straightforward application to angular-resolved MPI processes of molecules. For transparency of the presentation, we formulate the present theory for angular-resolved two-photon ionization (TPI) of a randomly oriented diatomic molecule (Sec. II) and consider in Sec. III the well-studied H_2 molecule as an explicit example. We conclude with a brief summary.

II. THEORY

The process relevant to the present study can be schematically represented as follows:

$$H_2(\Omega_0) + 2\gamma^q(\hbar\omega) \rightarrow H_2^+(\Omega_1) + e^-(\varepsilon\ell m\mu). \qquad (1)$$

A randomly orientated hydrogen molecule in its ground electronic state $1\sigma_g^2(X\,{}^1\Sigma_g^+)$ absorbs two linearly ($q = 0$) or circularly ($q = \pm 1$) polarized photons of energy ω. The event results in the molecular ion H_2^+ in its ground state $1\sigma_g^1(X\,{}^2\Sigma_g^+)$ and the outgoing photoelectron e^- with energy ε, which can be expanded in the asymptotical region via partial waves (see, e.g., Ref. [23]) with fixed projections m and μ of the orbital momentum ℓ and spin s, respectively.

---

[*] philipp.demekhin@pci.uni-heidelberg.de

We assume for simplicity that either Hund's coupling case (a) or (b) applies for the description of the diatomic molecule [24]. Therefore, an electronic state can be described by the projection of the total electronic angular momentum along the molecular axis, $\Omega = \Lambda + \Sigma$. We also neglect below the nuclear vibrational and rotational motions during the electronic transition, which were demonstrated to be of minor importance for TPI of H_2 [7–9]. Thus, the process is described as a vertical transition at the equilibrium internuclear distance of the ground electronic state $r_e = 0.74152$ Å [25].

A. Differential cross section

The angular distribution of photoelectrons is described by the well-known formula for the differential TPI cross section of randomly oriented diatomic molecules [7,9]:

$$\begin{aligned}\frac{d\sigma^q(\omega)}{d\Omega} &= \frac{1}{4\pi}\sum_{L=0,2,4} A_L^q(\omega) P_L(\cos\theta) \\ &= \frac{\sigma^q(\omega)}{4\pi}\left[1 + \beta_2^q(\omega)P_2(\cos\theta) + \beta_4^q(\omega)P_4(\cos\theta)\right].\end{aligned} \tag{2}$$

Here, θ is the angle between the direction of propagation of the outgoing electron emitted into the solid angle $d\Omega$ and the electric-field vector of linearly polarized light ($q = 0$), or the direction of propagation of circularly polarized light ($q = \pm1$); P_L are the Legendre polynomials; and the total TPI cross section σ^q and the angular distribution parameters β_2^q and β_4^q are defined as $\sigma^q = A_0^q$, $\beta_2^q = A_2^q/A_0^q$, and $\beta_4^q = A_4^q/A_0^q$, respectively.

The present approach to derive an analytical expression for the coefficients A_L^q in Eq. (2) is similar to that reported in Refs. [19,26]. We chose the quantization axis in the laboratory frame (z) along the electric-field vector for linearly polarized light (or along the propagation direction of circularly polarized light) and in the molecular frame (z') along the molecular axis. At first, two exciting photons $2\gamma^q$ with the polarization q given in the laboratory frame were transformed into the molecular frame. Then, the photoelectron partial waves $\varepsilon\ell m\mu$ with the quantum numbers defined in the molecular frame were transformed into the laboratory frame. Afterward, the differential cross section was averaged over all orientations of the molecular axis in the laboratory frame. We also assume that the spin polarization of the photoelectrons μ is not resolved in the experiment. All necessary equations for the transformations and further simplifications can be found elsewhere [23].

In the length form of the electric dipole transition operator, the final result for the coefficients A_L^q reads

$$\begin{aligned}A_L^q(\omega) = {}& \frac{4\pi^2\alpha a_0^2\omega}{g}\left(\frac{I}{I_0}\right)\sum_{\Omega_0\Omega_1}\sum_{\zeta\zeta'\mu}(i)^{\ell+\ell'}e^{i(\delta_{\ell m}-\delta_{\ell' m'})}\sqrt{(2\ell+1)(2\ell'+1)}\sum_{M_L}\sum_{JM_J}\sum_{KM_K}(2L+1) \\ &\times(2J+1)(2K+1)(-1)^{\ell'+L+m+k'+p'}\begin{pmatrix}\ell & \ell' & L\\ 0 & 0 & 0\end{pmatrix}\begin{pmatrix}\ell & \ell' & L\\ -m & m' & -M_L\end{pmatrix}\begin{pmatrix}1 & 1 & J\\ q & -q & 0\end{pmatrix} \\ &\times\begin{pmatrix}1 & 1 & J\\ p & -p' & -M_J\end{pmatrix}\begin{pmatrix}1 & 1 & K\\ k & -k' & -M_K\end{pmatrix}\begin{pmatrix}1 & 1 & K\\ q & -q & 0\end{pmatrix}\begin{pmatrix}J & K & L\\ M_J & M_K & M_L\end{pmatrix}\begin{pmatrix}J & K & L\\ 0 & 0 & 0\end{pmatrix} \\ &\times\langle\Omega_0|\mathbf{d}_{p'}\mathbf{d}_{k'}|\Omega_1\varepsilon\ell'm'\mu\rangle\langle\Omega_1\varepsilon\ell m\mu|\mathbf{d}_k\mathbf{d}_p|\Omega_0\rangle,\end{aligned} \tag{3}$$

where g is the statistical weight of the initial electronic state, $\alpha = 1/137.036$ is the fine-structure constant, a_0 is the Bohr radius, $\delta_{\ell m}$ is the phase shift of the electron partial wave, I is the radiation intensity, and $I_0 = 1.4038 \times 10^{17}$ W/cm^2. The energy of the photoelectron ε is connected with the photon energy ω and the ionization potential IP via $2\omega = V_{\text{ion}} + \varepsilon$. The first summation in Eq. (3) must be performed over all degenerate initial and final-ionic electron states of the diatomic molecule, and indices ζ and ζ' in the second summation run over all possible quantum numbers $\zeta = \{\ell mkp\}$.

From the third, sixth, and last $3j$ symbols in Eq. (3) it automatically follows that index L can only be equal to 0, 2, or 4 for any light polarization q. Indices p and k, which describe the polarizations of the first and second absorbed photons in the molecular frame (z' axis), may take any possible values among $0, \pm1$, and they are not necessarily identical. Therefore, two-photon ionization of the ground-state $1\sigma_g(m = 0)$ orbital of H_2 results generally in nine possible pathways:

$$\begin{tikzcd} & \sigma_u(0) \arrow[dr, "0"] & \\ \sigma_g(0) \arrow[ur, "0"] \arrow[dr, "\pm1"'] & & \sigma_g(0), \\ & \pi_u(\pm1) \arrow[ur, "\mp1"'] & \end{tikzcd} \tag{4a}$$

$$\begin{tikzcd} & \sigma_u(0) \arrow[dr, "\pm1"] & \\ \sigma_g(0) \arrow[ur, "0"] \arrow[dr, "\pm1"'] & & \pi_g(\pm1), \\ & \pi_u(\pm1) \arrow[ur, "0"'] & \end{tikzcd} \tag{4b}$$

$$\sigma_g(0) \overset{\pm1}{\rightarrow} \pi_u(\pm1) \overset{\pm1}{\rightarrow} \delta_g(\pm2). \tag{4c}$$

Three pathways in the $\varepsilon\sigma_g$ channel (4a) result in identical final states and superimpose. The same interference occurs for the two pathways in each of the $\varepsilon\pi_g$ channels (4b). Therefore, partial TPI cross sections for channels (4a) and (4b) contain coherent superpositions of the above mentioned pathways, described by Eq. (3).

B. Two-photon transition matrix element

The TPI matrix element is given in the lowest nonvanishing order of perturbation theory by

$$\langle\Omega_1\varepsilon\ell m\mu|\mathbf{d}_k\mathbf{d}_p|\Omega_0\rangle = \sum_R \frac{\langle\Omega_1\varepsilon\ell m\mu|\mathbf{d}_k|\Omega_R\rangle\langle\Omega_R|\mathbf{d}_p|\Omega_0\rangle}{E_R - E_0 - \omega}. \tag{5}$$

Summation in Eq. (5) is performed over all possible intermediate electronic states Ω_R with energy E_R in the discrete and continuous spectrum, which is a formidable task since the dipole transition amplitudes between two continuous states are diverging. The present approach to compute the matrix element (5) consists in introducing the so-called single-particle correlation function (see, e.g., Refs. [27,28]). For the TPI of H_2 in its ground electronic state $|\Omega_0\rangle = 1\sigma_g^2(^1\Sigma_g^+)$, the correlation function is defined by

$$|\Psi_p^c(\omega)\rangle = \sum_{\varepsilon} \frac{|\varepsilon\lambda_u\rangle\sqrt{2}\langle\varepsilon\lambda_u|\mathbf{d}_p|1\sigma_g\rangle}{V_{\rm ion}+\varepsilon-\omega}, \qquad (6)$$

where $V_{\rm ion}+\varepsilon$ stands for the energy difference $E_R - E_0$. The correlation function depends on the photon energy ω and also on the polarization p of the first photon in the molecular frame. The symmetry λ of virtual molecular orbital (MO) $|\varepsilon\lambda_u\rangle$ is determined by this polarization via the selection rules for the dipole transitions: The linear polarization $p = 0$ results in the transition to the $|\varepsilon\sigma_u\rangle$ orbital, and circular polarization $p = \pm 1$ results in the transition to the $|\varepsilon\pi_u\rangle$ one. These virtual orbitals form singlet intermediate states $|\Omega_R\rangle = 1\sigma_g^1\varepsilon\sigma_u^1(^1\Sigma_u^+)$ or $1\sigma_g^1\varepsilon\pi_u^1(^1\Pi_u)$, respectively. The factor $\sqrt{2}$ in Eq. (6) arises from the antisymmetrization of the singlet state $|\Omega_R\rangle$.

The matrix element (5) can now be computed according to

$$\langle\Omega_1\varepsilon\ell m\mu|\mathbf{d}_k\mathbf{d}_p|\Omega_0\rangle = \langle\varepsilon\ell m|\mathbf{d}_k|\Psi_p^c\rangle. \qquad (7)$$

By introducing the one-particle Hamiltonian for an optically exited electron, $\mathbf{h}|\varepsilon\lambda_u\rangle = \varepsilon|\varepsilon\lambda_u\rangle$, and implying the resolution of the identity, $\sum_\varepsilon |\varepsilon\lambda_u\rangle\langle\varepsilon\lambda_u| = 1$, we arrive at the following inhomogeneous equation for the correlation function:

$$\begin{aligned}[\mathbf{h} + V_{\rm ion} - \omega]\big|\Psi_p^c(\omega)\big\rangle &= \sum_{\varepsilon} |\varepsilon\lambda_u\rangle\sqrt{2}\langle\varepsilon\lambda_u|\mathbf{d}_p|1\sigma_g\rangle \\ &= \sqrt{2}\,\mathbf{d}_p|1\sigma_g\rangle. \qquad (8)\end{aligned}$$

Because of the inhomogeneous character of Eq. (8) it can be solved at any photon energy ω. In the present work, we are interested in the below-threshold TPI (i.e., $\omega < V_{\rm ion}$). Therefore, the correlation function (6) has a discrete-type localization (see also Fig. 4), and, except those photon energies which exactly correspond to the positions of optical resonances $\omega_R = E_R - E_0$, the dipole integral (7) does not diverge [27,28]. The correlation function technique is somewhat similar to the commonly applied Green's-function approach (see, e.g, Refs. [7–9]).

C. Molecular wave functions

The occupied molecular orbitals were computed within the MO LCAO approach, whereas the single center method [15,16,19] with precise numerical molecular-field potentials was applied in order to compute both the correlation functions and the mutually orthogonal observable incoming partial photoelectron waves. According to the SC method the MO of a diatomic molecule is represented as an expansion by spherical harmonics, $Y_{\ell m}(\theta,\varphi)$, with respect to the center:

$$\Psi_{nm}(x,y,z) = \sum_{\ell} \frac{P_{n\ell m}(r)}{r} Y_{\ell m}(\theta,\varphi), \qquad (9)$$

where $P_{n\ell m}(r)$ stands for the radial parts of the partial harmonics in the SC expansion. The radial parts $P_{n\ell m}(r)$ of the photoelectron MO satisfy the following system of coupled differential Hartree-Fock equations [15,16]:

$$\begin{aligned}\sum_{\ell'}\Bigg\{&\left[-\frac{1}{2}\frac{d^2}{dr^2} + \frac{\ell(\ell+1)}{2r^2} - \varepsilon_{nm}\right]\delta_{\ell\ell'} + V^{\rm ne}_{\ell\ell'}(r) \\ &+ V^{ee}_{\ell\ell'}(r)\Bigg\} P_{n\ell' m}(r) = 0. \qquad (10)\end{aligned}$$

In the system of Eqs. (10) the following designations are used: ε_{nm} is the one-electron energy in atomic units, $V^{\rm ne}_{\ell\ell'}(r)$ is the potential describing nuclear-electron interaction, and

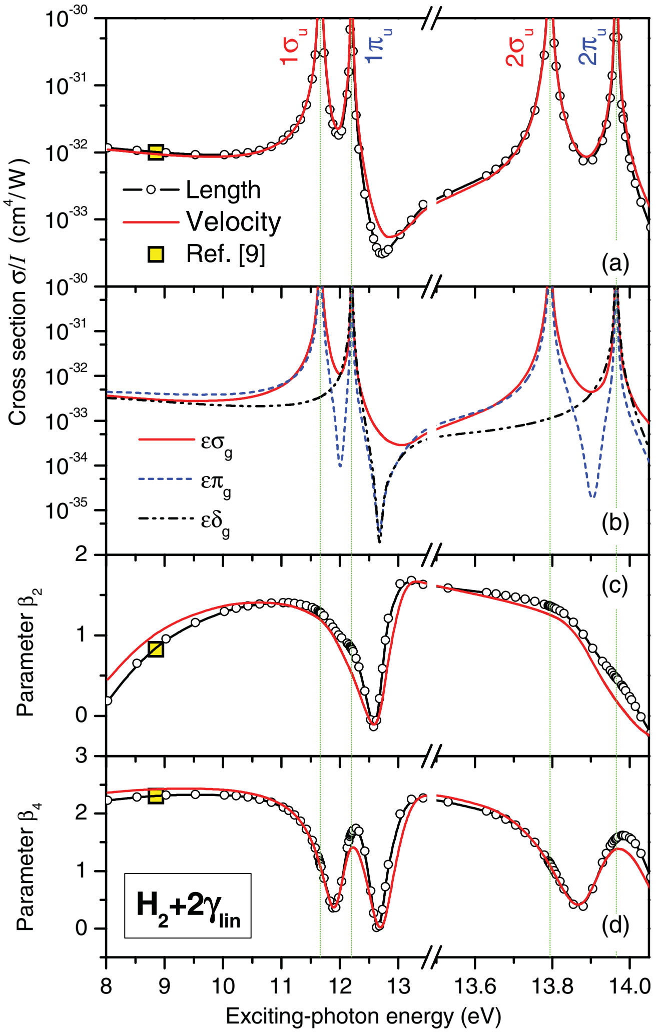

FIG. 1. (Color online) Two-photon ionization of H_2 by linearly polarized light. Shown are the (a) total cross sections $\sigma^0(\omega)/I$ and the photoelectron angular distribution parameters (c) $\beta_2^0(\omega)$ and (d) $\beta_4^0(\omega)$ computed in the length (open circles) and velocity (solid curves) gauges. Theoretical results from Ref. [9] obtained at the photon energy of 8.854 eV are depicted by open squares. Partial cross sections (b) are shown in the length gauge only. Note the two different energy scales below and above 13.5 eV. At the exact positions of the optical resonances (indicated by vertical lines), the presently computed cross sections diverge, since the TPI matrix element (5) does not account for lifetimes of the resonances [see discussion in the text before Eq. (11)].

$V^{ee}_{\ell\ell'}(r)$ is the potential describing direct and exchange electrostatic Coulomb interactions of the photoelectron with the ionic core. These potentials were calculated using the LCAO of the ground-state MOs deconvolved as Eq. (9). The method for numerically solving the system of integrodifferential Eqs. (10) in the discrete and continuous spectrum is described in detail in Ref. [16].

III. RESULTS AND DISCUSSIONS

The present calculations have been performed in the length and velocity form of the electric dipole transition operator. The experimental vertical ionization potential of the H_2 molecule, $V_{\rm ion} = 15.43$ eV [29], was used in the calculations. The angular-resolved TPI spectra of H_2 computed for linearly and circularly polarized exciting radiation are depicted in Figs. 1 and 2, respectively. The exciting-photon energy interval chosen for the present calculations covers the four lowest optical resonant states of the molecule accessible by the first photon from the ground electronic state, i.e., the $1\sigma_g^1 1\sigma_u^1 (B\,^1\Sigma_u^+)$, $1\sigma_g^1 1\pi_u^1 (C\,^1\Pi_u)$, $1\sigma_g^1 2\sigma_u^1 (B'\,^1\Sigma_u^+)$, and $1\sigma_g^1 2\pi_u^1 (D\,^1\Pi_u)$ resonances [25].

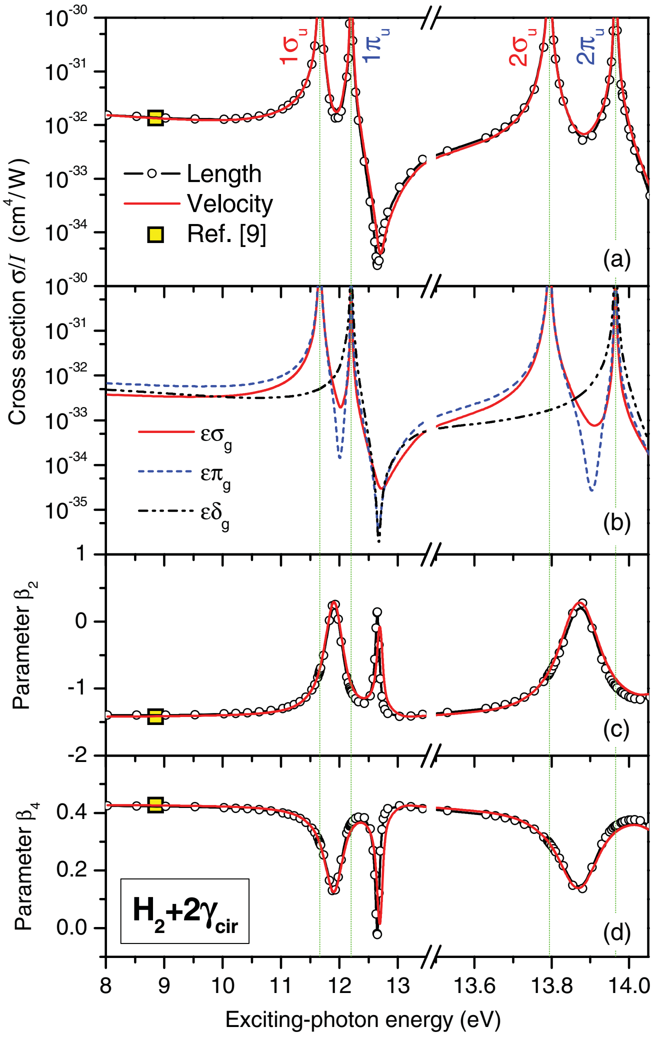

FIG. 2. (Color online) Two-photon ionization of H_2 by circularly polarized light. See notations in Fig. 1.

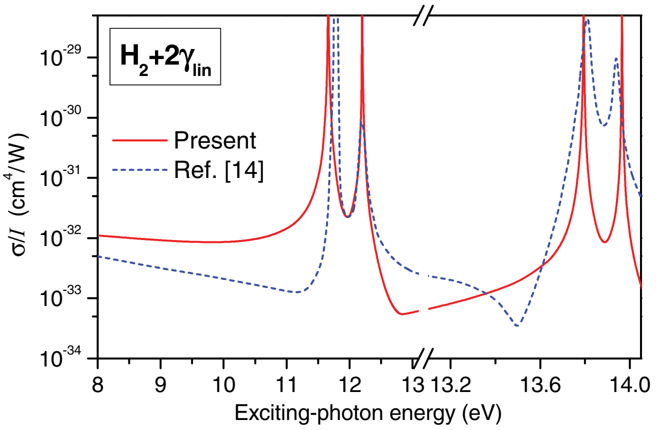

FIG. 3. (Color online) Two-photon ionization of H_2 by linearly polarized light. Solid curve: present results from Fig. 1 in velocity form. Broken curve: theoretical results from Ref. [14] in velocity form. The generalized cross section from Ref. [14] was converted in cm^4/W units as described in the text and, for a better comparison, shifted by −0.85 eV.

In Figs. 1 and 2, the absolute total and partial TPI cross sections normalized to the radiation intensity (i.e., $\sigma^q(\omega)/I$) are collected in panels (a) and (b), respectively, whereas the angular distribution parameters $\beta_2(\omega)$ and $\beta_4(\omega)$ are depicted in panels (c) and (d), respectively. The cross sections and angular distribution parameters computed in the length (open circles) and velocity (solid curves) form of the electric dipole transition operator are very close to each other, which indicates a reliability of the present calculation. The present results are also in excellent agreement with the single theoretical result from Ref. [9] obtained at $\omega = 8.854$ eV in the length gauge (open squares).

In Fig. 3, the presently computed total cross section for TPI by linearly polarized light is compared with the theoretical results from Ref. [14]. In order to convert the generalized cross section depicted in Fig. 6(a) of Ref. [14] in cm^{4}s^1 units, the latter was divided by the photon energy ω measured in Joule units (27.2114 eV = 4.3597×10^{-18} J). In addition, it was shifted in energy by −0.85 eV for a better comparison. An overall qualitative agreement between the two computed cross sections is seen from Fig. 3, but a noticeable quantitative difference exists. The latter disagreement could be connected with different theoretical approaches applied.

At the exact energy positions $\omega_R = E_R - E_0$ of the optical resonances $|R\rangle$, the presently computed cross sections diverge (see Figs. 1 and 2). This is because the energy detuning $E_R - E_0 - \omega_R$ in the denominator of the TPI amplitude [Eq. (5)] becomes zero. As a consequence, the correlation function (6) diverges. In the present theoretical formulation (second order of the perturbation theory), the exciting radiation is assumed to be perfectly monochromatized, and all intermediate optical resonances are treated as stationary states. In a more accurate treatment, optical resonances are transient with the lifetimes given by their radiative decay and also by the strong-field ionization [30]. In addition, they are broadened by a bandwidth of the exciting photons.

In order to incorporate the latter processes in the theory, one has to introduce the total width of the optical resonance Γ_R and to modify the energy denominator of Eq. (5) by an

TABLE I. Parameters f_R^q [Eq. (12)] computed for the TPI of H_2 via a given intermediate resonant state $|R\rangle$ in $\text{cm}^4/\text{W}E_h^2$ units, where $E_h = 1$ a.u. of energy. The presently computed one-electron energy ε_R of the excited orbital, the resonant photon energy $\omega_R = V_{\text{ion}} + \varepsilon_R$ (where $V_{\text{ion}} = 15.43$ eV [29]), and the experimental [25] energy position of the resonances E^{expt} are also indicated.

$\vert R\rangle$	ε_R (eV)	ω_R (eV)	E^{expt} (eV)	f_R^0 (length)	f_R^0 (velocity)	f_R^1 (length)	f_R^1 (velocity)
$1\sigma_u$	−3.767	11.663	11.369	0.214×10^{-35}	0.226×10^{-35}	0.205×10^{-35}	0.209×10^{-35}
$1\pi_u$	−3.229	12.201	12.410	0.388×10^{-36}	0.553×10^{-36}	0.444×10^{-36}	0.572×10^{-36}
$2\sigma_u$	−1.635	13.795	13.842	0.700×10^{-37}	0.674×10^{-37}	0.669×10^{-37}	0.625×10^{-37}
$2\pi_u$	−1.465	13.965	14.124	0.174×10^{-37}	0.229×10^{-37}	0.193×10^{-37}	0.237×10^{-37}

additional imaginary term $+\frac{i}{2}\Gamma_R$ (see, e.g., Refs. [30,31]). In the vicinity of a transient intermediate resonance $|R\rangle$, the TPI cross section can be parameterized by

$$\frac{\sigma^q(\omega)}{I} = \frac{f_R^q}{(\omega_R-\omega)^2+(\Gamma_R/2)^2}. \tag{11}$$

Parameters f_R^q in the numerator of Eq. (11) can be obtained from Eq. (3) by setting $L = 0$ and replacing the TPI matrix element $\langle\Omega_1\varepsilon\ell m\mu|\mathbf{d}_k\mathbf{d}_p|\Omega_0\rangle$ by the product of two matrix elements for the excitation of the energy-selected optical resonance $\langle R|\mathbf{d}_p|\Omega_0\rangle$ and its subsequent ionization $\langle\Omega_1\varepsilon\ell m\mu|\mathbf{d}_k|R\rangle$. After simplifications, an explicit expression for f_R^q reads

$$f_R^q = \frac{4\pi^2\alpha a_0^2\omega}{gI_0}\sum_{\Omega_0\Omega_1}\sum_{\ell m\mu}\sum_{kp}\sum_{k'p'}\sum_{J}(-1)^{k'+p}(2J+1)\begin{pmatrix}1 & 1 & J\\ p & -p' & k-k'\end{pmatrix}\begin{pmatrix}1 & 1 & J\\ k & -k' & p-p'\end{pmatrix}$$
$$\times\begin{pmatrix}1 & 1 & J\\ q & -q & 0\end{pmatrix}^2\langle\Omega_0|\mathbf{d}_{p'}|R\rangle\langle R|\mathbf{d}_{k'}|\Omega_1\varepsilon\ell m\mu\rangle\langle\Omega_1\varepsilon\ell m\mu|\mathbf{d}_k|R\rangle\langle R|\mathbf{d}_p|\Omega_0\rangle. \tag{12}$$

The parameters f_R^q computed within the SC method for the TPI of H_2 via the optical resonant states $|R\rangle$ are listed in Table I in $\text{cm}^4/\text{W}E_h^2$ units. Computed SC one-electron energies ε_R of the excited resonant states and the resonant photon energies $\omega_R = V_{\text{ion}} + \varepsilon_R$ are also indicated in columns 2 and 3 of Table I. One can see that the presently computed energy positions of the optical resonances ω_R are in a good agreement with the experimental energies E^{expt} from Ref. [25] (cf. columns 3 and 4). Using the presently computed values of f_R^q and ω_R from Table I, one can obtain [via Eq. (11)] the theoretical cross sections in the vicinity of $|R\rangle$ for any known total width of the optical resonance Γ_R.

Let us now turn to the computed angular distribution parameters $\beta_2^q(\omega)$ and $\beta_4^q(\omega)$ depicted in panels (c) and (d) of Figs. 1 and 2. In contrast to the cross sections, the parameters show no dramatic changes in the close proximities of the optical resonances (indicated by vertical lines). However, their exciting-photon energy dependencies exhibit prominent resonant features in the vicinities of minima in the total cross section. This is because the β parameters are inversely proportional to the cross section, i.e., $\beta_L^q \sim (\sigma^q)^{-1}$, and small changes in the cross section around its minimum cause large changes in the angular distribution [32].

The minima in the cross section appear as the result of a destructive interference of the amplitudes for the ionization via two neighboring intermediate resonances. Therefore, these minima and, as a consequence, resonant features in β parameters, are located in between the resonances (see Figs. 1 and 2). As also seen from panels (b) of the figures, the destructive interference is manifested differently in the partial cross sections for the channels (4a)–(4c). For the $\varepsilon\pi_g$ and $\varepsilon\delta_g$ channels these minima are significantly deeper than those for the $\varepsilon\sigma_g$ channel. The resonant features in the angular distribution parameters provide a very sensitive tool to study interplay between the partial ionization channels (4) around the minima in the cross sections.

Finally, in Fig. 4 we show by solid curves several SC partial harmonics of the correlation function (6) computed at $\omega = 11.6625$ eV, which is very close but does not coincide with the energy for the first optical resonance $1\sigma_g^1 1\sigma_u^1(B\,^1\Sigma_u^+)$ ($\omega_R =$

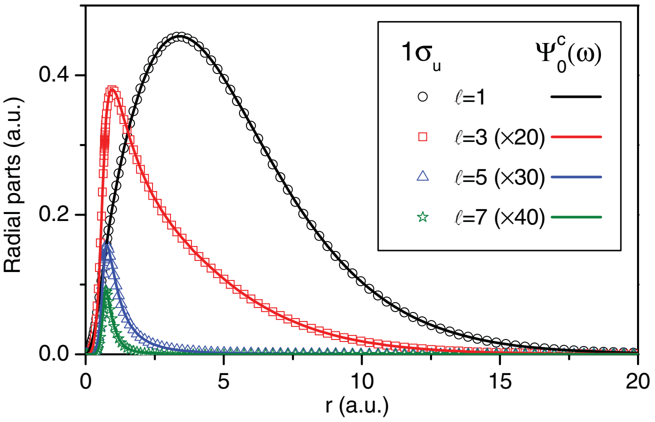

FIG. 4. (Color online) Wave function of the $1\sigma_u$ excited electron (open symbols) and the correlation function (solid curves) computed in the vicinity of the first optical resonance at $\omega = 11.6625$ eV (the energy detuning from the resonance amounts to −0.5 meV). The latter is normalized to unity. Note that higher partial harmonics are shown on enhanced scales indicated by factors $\times K$.

11.663 eV, see Table I). The norm of the function was set to one. The respective partial harmonics of the SC expansion of the $1\sigma_u$ MO are also presented in the figure by open symbols. As was expected and also seen from Fig. 4, this normalized correlation function coincides with the wave function of the $1\sigma_u$-excited electron. As was already mentioned in Sec. II B, solutions of the inhomogeneous Eq. (8) for any $\omega < V_{\text{ion}}$ belong to the discrete spectrum of the one-electron Hamiltonian $\mathbf{h}$, and, thus, they are localized in space. By its definition [Eq. (6)], the correlation function is inversely proportional to the energy detuning $\Psi_p^c(\omega) \sim (E_R - E_0 - \omega)^{-1}$ and is diverging at the exact position of the resonance. In order to eliminate this divergence, one has to account for the transient character of the optical resonance by introducing the imaginary term $+\frac{i}{2}\Gamma_R$ in the energy denominator of Eq. (6) and also in the left-hand side of Eq. (8).

IV. CONCLUSIONS

Two-photon ionization of the H_2 molecule is studied theoretically in the exciting-photon energy range of 8–14 eV. The theoretical approach is based on the combination of the single center method, for accurate computation of discrete molecular orbitals and continuous partial photoelectron waves, and the correlation function technique, to evaluate numerically the two-photon transition matrix elements. Thereby, it is especially designed to study angular-resolved two-photon ionization spectra of diatomic molecules. The method also allows a straightforward extension to multiphoton ionization processes of diatomic and also polyatomic molecules.

Cross sections and angular distribution parameters for the two-photon ionization of H_2 by linearly and circularly polarized radiation computed in the length and velocity forms of the electric dipole transition operator are very close to each other, and they also agree well with the other available theoretical results. Our calculations predict strong exciting-photon energy dependencies of the angular distribution parameters in the vicinities of minima in the total cross section in between two neighboring optical resonances. We note that the nuclear dynamics during the ionization process, neglected in the present calculations, will result in a slight broadening of the presently computed spectra. Computed exciting-photon energy dependencies of the cross sections and angular distribution parameters provide reliable benchmarks for available computational approaches and for further angular-resolved multiphoton ionization experiments on the hydrogen molecule.

[1] D. M. Friedrich and W. M. McClain, Annu. Rev. Phys. Chem. **31**, 559 (1980).

[2] P. M. Johnson and C. E. Otis, Annu. Rev. Phys. Chem. **32**, 139 (1981); P. M. Johnson, Appl. Opt. **19**, 3920 (1980).

[3] M. Stuke, Ber. Bunsen-Ges. Phys. Chem. **86**, 837 (1982).

[4] J. A. Syage and J. Wessel, Appl. Spectr. Rev. **24**, 1 (1988).

[5] R. Bruzzese, A. Sasso, and S. Solimeno, Riv. Nuovo Cimento **12**, 1 (1989).

[6] K. P. Aicher, U. Wilhelm, and J. Grotemeyer, J. Am. Soc. Mass. Spectrom. **6**, 1059 (1995).

[7] V. A. Davidkin and L. P. Rapoport, J. Phys. B **7**, 1101 (1974).

[8] V. A. Davidkin and L. P. Rapoport, Kvantovaya Elektron. **2**, 343 (1975); Sov. J. Quantum Electron. **5**, 195 (1975).

[9] B. Ritchie and E. J. McGuire, Phys. Rev. A **24**, 2532 (1981).

[10] P. G. Burke, J. Colgan, D. H. Glass, and K. Higgins, J. Phys. B **33**, 143 (2000).

[11] H. Bachau, J. Phys. B **35**, 509 (2002).

[12] S. Barmaki, S. Laulan, H. Bachau, and M. Ghalim, J. Phys. B **36**, 817 (2003).

[13] A. Apalategui, A. Saenz, and P. Lambropoulos, J. Phys. B **33**, 2791 (2000).

[14] A. Apalategui and A. Saenz, J. Phys. B **35**, 1909 (2002).

[15] Ph. V. Demekhin, D. V. Omelyanenko, B. M. Lagutin, V. L. Sukhorukov, L. Werner, A. Ehresmann, K. H. Schartner, and H. Schmoranzer, Opt. Spektrosk. **102**, 318 (2007).

[16] Ph. V. Demekhin, A. Ehresmann, and V. L. Sukhorukov, J. Chem. Phys. **134**, 024113 (2011).

[17] D. M. Bishop, Adv. Quantum Chem. **3**, 25 (1967).

[18] V. L. Sukhorukov, V. F. Demekhin, V. A. Yavna, I. D. Petrov, L. A. Demekhina, and S. V. Lavrentiev, Koord. Khim. (Sov.) **9**, 158 (1983).

[19] Ph. V. Demekhin, I. D. Petrov, V. L. Sukhorukov, W. Kielich, P. Reiss, R. Hentges, I. Haar, H. Schmoranzer, and A. Ehresmann, Phys. Rev. A **80**, 063425 (2009); **81**, 069902(E) (2010).

[20] Ph. V. Demekhin, I. D. Petrov, T. Tanaka, M. Hoshino, H. Tanaka, K. Ueda, W. Kielich, and A. Ehresmann, J. Phys. B **43**, 065102 (2010).

[21] Ph. V. Demekhin, I. D. Petrov, V. L. Sukhorukov, W. Kielich, A. Knie, H. Schmoranzer, and A. Ehresmann, Phys. Rev. Lett. **104**, 243001 (2010).

[22] Ph. V. Demekhin, I. D. Petrov, V. L. Sukhorukov, W. Kielich, A. Knie, H. Schmoranzer, and A. Ehresmann, J. Phys. B **43**, 165103 (2010).

[23] N. A. Cherepkov, J. Phys. B **14**, 2165 (1981).

[24] G. Herzberg, *Molecular Spectra and Molecular Structure: I. Spectra of Diatomic Molecules* (Van Nostrand Reinhold Comp., New York, 1950).

[25] K. P. Huber and G. Herzberg, *Molecular Spectra and Molecular Structure. IV. Constants of Diatomic Molecules* (Van Nostrand Reinhold, New York, 1979).

[26] Ph. V. Demekhin, I. D. Petrov, and A. Ehresmann, Phys. Rev. A **82**, 041401(R) (2010).

[27] S. L. Carter and H. P. Kelly, Phys. Rev. A **16**, 1525 (1977).

[28] V. L. Sukhorukov, B. M. Lagutin, I. D. Petrov, H. Schmoranzer, A. Ehresmann, and K. H. Schartner, J. Phys. B **27**, 241 (1994).

[29] *NIST Electron Impact Cross Sections for Ionization and Excitation of Molecules* (National Institute of Standards and Technology, Gaithersburg, MD, 2011), [http://physics.nist.gov/PhysRefData/Ionization/molTable.html].

[30] N. B. Delone and V. P. Krainov, *Multiphoton Processes in Atoms* (Springer, Heidelberg, 2000), 2nd ed.

[31] P. Cremaschi, P. M. Johnson, and J. L. Whitten, J. Chem. Phys. **69**, 4341 (1978).

[32] B. M. Lagutin, Ph. V. Demekhin, I. D. Petrov, V. L. Sukhorukov, A. Ehresmann, F. Voliweiler, H. Schmoranzer, and K.-H. Schartner, J. Struct. Chem. **39**, 811 (1998).